# $^{18}$F-Fluoromisonidazole PET/CT: A Potential Tool for Predicting Primary Endocrine Therapy Resistance in Breast Cancer

Jingyi Cheng*[1,2], Li Lei*[3,4], Junyan Xu[1,2], Yifei Sun[1,2], Yongping Zhang[1,2], Xincun Wang[1,2], Lingling Pan[1,2], Zhimin Shao[3,4], Yingjian Zhang[1,2], and Guangyu Liu[3,4]

*[1]Department of Nuclear Medicine, Fudan University Shanghai Cancer Center, Shanghai, China; [2]Department of Oncology, Shanghai Medical College, Fudan University, Shanghai, China; [3]Department of Breast Surgery, Fudan University Shanghai Cancer Center, Shanghai, China; and [4]Department of Oncology, Shanghai Medical College, Fudan University, Shanghai, China*

Although endocrine therapy is an effective method to treat estrogen receptor (ER)–positive breast cancer, approximately 30%–40% of all hormone receptor–positive tumors display de novo resistance. The aim of our current study was to analyze whether $^{18}$F-labeled fluoromisonidazole (1-(2-nitro-1-imidazolyl)-2-hydroxy-3-fluoropropane [$^{18}$F-FMISO]) PET/CT could predict primary resistance to hormonal therapy in ER-positive breast cancer. **Methods:** Postmenopausal women who had ER-α–positive breast cancer, stages II–IV, and had never received prior endocrine therapy were prospectively enrolled in this study. Patients underwent both $^{18}$F-FDG and $^{18}$F-FMISO PET/CT scans before and after treatment. The hottest $^{18}$F-FDG standardized uptake value (SUV) in the tumor foci, the SUVs at 2 and 4 h, and the TBR2 h and TBR4 h for the target lesions were calculated (TBR2 h = SUV2 $h_T$/SUV2 $h_B$ and TBR4 h = SUV4 $h_T$/SUV4 $h_B$ [TBR is the tumor-to-background ratio]). Clinical outcomes of primary endocrine therapy with letrozole were evaluated according to the criteria of the World Health Organization after at least 3 mo of treatment. Immunohistochemistry for markers of proliferation (Ki67) and hypoxia-induced factor 1α was performed on a subset of tumors that had undergone biopsy or surgery. Pearson and Spearman analysis was used to determine the correlation between the parameters of $^{18}$F-FDG and $^{18}$F-FMISO uptake and clinical or immunohistochemistry outcomes with a 0.01 threshold for statistical significance. **Results:** A total of 45 lesions (13 primary, 32 metastatic) from 20 patients met the inclusion criteria in this study. Baseline $^{18}$F-FDG and $^{18}$F-FMISO PET/CT scans were obtained for 33 lesions from 16 patients. The correlation between baseline $^{18}$F-FDG uptake and clinical outcome was weak and did not reach statistical significance ($r$ = 0.37, $P$ = 0.031). However, there was a significantly positive correlation between baseline $^{18}$F-FMISO uptake (SUV2 $h_T$, TBR2 h, SUV4 $h_T$, and TBR4 h) and clinical outcomes after ≥3 mo of primary endocrine therapy with letrozole ($r$ = 0.77, 0.76, 0.71, and 0.78, respectively; $P < 0.0001$). The application of a TBR4 h cutoff of ≥1.2 allowed the prediction of 88% of the cases of progressive disease (15/17). Despite poor correlation between $^{18}$F-FMISO uptake and hypoxia-induced factor 1α expression, a marginal positive correlation between TBR4 h and Ki67 expression was measured ($r$ = 0.51, $P$ = 0.011) in a subset of malignant lesions acquired by biopsy or surgery. **Conclusion:** $^{18}$F-FMISO PET/CT can be used to predict primary endocrine resistance in ER-positive breast cancer.

**Key Words:** hypoxia; breast cancer; $^{18}$F-FMISO; hormonal therapy; resistance

**J Nucl Med 2013; 54:333–340**
DOI: 10.2967/jnumed.112.111963

Approximately 70% of breast carcinomas are hormone-dependent and overexpress hormone receptors, such as estrogen receptor (ER)-α. As a result, endocrine therapy has emerged as an important tool to treat ER-positive breast cancer. New-generation hormonal therapy (e.g., third-generation aromatase inhibitors) has performed better than traditional antiestrogen therapy (i.e., tamoxifen) in both early-stage and advanced breast cancer in postmenopausal women (*1*). However, approximately 30% of ER-positive breast cancer will unfortunately display primary resistance to hormonal therapy (*2*), and some may develop acquired resistance to the therapy after initial treatment (*1*).

Hypoxia is a normal phenomenon in solid tumors that arises, in part, from uncontrolled proliferation and immature blood vessels (*3*). Previous studies have demonstrated that hypoxia and its biomarker, hypoxia-induced factor (HIF), are strongly associated with tumor propagation, malignant progression, and resistance to anticancer treatments, such as radiotherapy (*4–6*). Kurebayashi et al. (*7*) first reported that hypoxia significantly reduced both the growth-promoting effects of estradiol (E2) and the growth-inhibitory effects of an antiestrogen on ER-positive breast cancer cell lines. Cooper et al. (*8*) observed that regional loss of ER-α expression was consistently present in

Received Jul. 27, 2012; revision accepted Sep. 26, 2012.
For correspondence or reprints contact: Guangyu Liu, Department of Breast Surgery, Fudan University Shanghai Cancer Center, and Department of Oncology, Shanghai Medical College, Fudan University, 399 Ling Ling Rd., Shanghai, China, 200032.
E-mail: liugy123@yahoo.com
*Contributed equally to this work.
Published online Feb. 11, 2013

hypoxic regions of breast cancer tissue. A recent study comparing neoadjuvant letrozole with letrozole plus metronomic cyclophosphamide found that increased levels of HIF-1α (Novus Biologicals) were significantly associated with resistance to treatment (*9,10*). Taken together, these data indicate that hypoxia might be associated with endocrine resistance in breast cancer.

In 1991, the gold standard—an $O_2$-sensitive electrode—was first used to measure breast tumors, and 40% of the tumors investigated contained hypoxic areas (*11*). Unfortunately, this method is invasive, indirect, and overall too restricted to become a tool for general clinical practice. With PET/CT, radiolabeled hypoxia-avid compounds can be applied to evaluate oxygenation status in experimental or human tumors. $^{18}$F-labeled fluoromisonidazole (1-[2-nitro-1-imidazolyl]-2-hydroxy-3-fluoropropane [$^{18}$F-FMISO]) is the most widely used nitroimidazole derivative in clinical PET/CT. Because $^{18}$F-FMISO has affinity only for hypoxic cells with functional nitroreductase enzymes, $^{18}$F-FMISO accumulates in activated cells but not in necrotic cells (*12*). In vivo animal model studies have shown that intracellular retention of $^{18}$F-FMISO depends on oxygen concentration, and the rate of $^{18}$F-FMISO binding under hypoxic conditions can be up to 28 times greater than binding under normoxic conditions (*13*). Many clinical studies have demonstrated an excellent correlation between the $^{18}$F-FMISO uptake and oxygenation status of gliomas, non–small cell lung cancer, head and neck cancer, and cervical cancer (*14–20*).

The major aim of our study was to analyze uptake of $^{18}$F-FMISO in ER-positive breast cancers, which are usually treated with endocrine therapy, and to predict primary endocrine resistance according to baseline $^{18}$F-FMISO PET/CT scans in breast cancer.

## MATERIALS AND METHODS

### Patients and Treatment

Postmenopausal women (mean age, 65.1 y; age range, 55–82 y) who had ER-α–positive breast cancer at stages II–IV and had never received prior endocrine therapy were considered eligible for this study. Patients were assigned to primary aromatase inhibitor treatment with letrozole (Femara; Novartis Pharmaceuticals Corp.), at 2.5 mg daily for at least 3 mo. Primary sites within the breast were assessed by ultrasound or MRI, and distant metastases were assessed by CT. Tumor response was evaluated according to the criteria of the World Health Organization (*21*). This prospective study was approved by the local ethics committee. Written informed consent was obtained from each candidate patient.

### PET/CT Scans

*PET/CT Protocol.* The baseline $^{18}$F-FDG/$^{18}$F-FMISO PET/CT scans were scheduled before initiation of endocrine therapy. The follow-up $^{18}$F-FDG/$^{18}$F-FMISO PET/CT scans were scheduled at least 3 mo later, just after the clinical evaluation for the tumor response to primary endocrine therapy. All PET/CT scans were obtained on a Biograph 16HR PET/CT (Siemens) operating in 3-dimensional, high-resolution mode. All emission images were reconstructed with a gaussian-filter iterative reconstruction method (iterations, 4; subsets, 8; image size, 168; filter, full width at half maximum, 5 mm) after corrections for scatter, singles, and random events, resulting in a spatial resolution of approximately 5 mm. The tomograph is regularly calibrated to convert counts per minute per pixel to megabecquerels per milliliter using large vials containing known activities of $^{18}$F imaged separately from the patient and reconstructed using the same filter as the emission images.

*$^{18}$F-FMISO Static PET/CT Scan.* $^{18}$F-FMISO was produced by a cyclotron (RDS Eclips ST; Siemens CTI) and an Explora FDG4 (Siemens) module using 1-(2′-nitro-1′-imidazolyl)-2-*O*-tetrahydropyranyl-3-*O*-tosyl-propanediol as a labeling precursor. $^{18}$F-FMISO PET/CT scans were acquired 2 or 3 d after the initial $^{18}$F-FDG PET/CT scan. All patients were injected intravenously with 370 MBq of $^{18}$F-FMISO. At 2 and 4 h after injection, static emission scans were obtained. The data acquisition procedure was as follows: CT was first performed with 120 kV, CARE Dose (Siemens) 4-dimensional mode, 80–250 mA, and a pitch of 3.6. Immediately after CT, a PET emission scan that covered the identical transverse field of view was obtained. The acquisition time was 5 min per table position. PET scans were processed using iterative reconstruction and measured attenuation correction.

*$^{18}$F-FDG PET/CT Whole-Body Scan.* $^{18}$F-FDG was produced automatically by a cyclotron (RDS Eclips ST; Siemens) and an Explora FDG4 module (Siemens) in our center. All patients were required to fast for at least 6 h to ensure glucose blood levels below 10 mmol/L. Before and after injection, patients were kept lying comfortably in a quiet, dimly lit room. Scanning was initiated 1 h after administration of the tracer (7.4 MBq/kg). The data acquisition procedure was as follows: CT was first performed, from the proximal thighs to head, with 120 kV, CARE Dose 4-dimensional mode, 80–250 mA, and a pitch of 3.6. Immediately after CT, a PET emission scan that covered the identical transverse field of view was obtained. The acquisition time was 2–3 min per table position. PET image datasets were reconstructed iteratively by application of the CT data for attenuation correction, and coregistered images were displayed on a workstation.

*Image Analysis.* Several lesions were evaluated, including primary lesions within the breast, regional lymph node metastases, local recurrences, and lung and pleura metastases. $^{18}$F-FDG/$^{18}$F-FMISO datasets were reconstructed using the attenuation maps provided by the low-dose CT dataset measured immediately before $^{18}$F-FDG/$^{18}$F-FMISO image acquisition at the same scanner. All images were analyzed on a clinical Leonardo workstation with TrueD software. All PET/CT acquisitions from a given $^{18}$F-FDG/$^{18}$F-FMISO sequence were coregistered with automatic methods using the $^{18}$F-FDG PET/CT scans as a reference. An elliptic volume of interest (VOI) was drawn manually around areas with abnormal $^{18}$F-FDG uptake to calculate $SUV_{peak}$ (the hottest spot in the tumor foci). Finally, 40% of the maximum $SUV_{peak}$ threshold was applied to delineate $VOI_{40}$, which was then pasted onto the $^{18}$F-FMISO PET/CT images to measure $SUV_{peak}$ for $^{18}$F-FMISO uptake. When a significant activity could not be visually distinguished by an experienced nuclear medicine physician, the $SUV_{peak}$ was calculated in the $VOI_{40}$ drawn on the initial PET/CT scan. This occurred when no $^{18}$F-FMISO uptake was visible in a $VOI_{40}$. When the initial $^{18}$F-FDG hypermetabolism disappeared on the PET/CT acquisition, the $VOI_{40}$ at initial data was copied onto the images at follow-up. The peak values in $^{18}$F-FMISO PET/CT images at 2 and 4 h were noted as SUV2 $h_T$ and SUV4 $h_T$. Additionally, six 0.5 × 0.5 × 0.5 cm small spheres (background) were located at the triceps brachii muscles, the scapula muscles, and the latissimus dorsi muscles both in the homon-

**TABLE 1**
Patient Characteristics and Imaging Data

| Patient no | Age (y) | Diagnoses | EP | PR | Baseline | | | | | Follow-up | | | | | Outcome |
|---|---|---|---|---|---|---|---|---|---|---|---|---|---|---|---|
| | | | | | Ki67 (%) | HIF-1α score | SUVFDGpeak | TBR2 h | TBR4 h | Ki67 (%) | HIF-1α score | SUVFDG peak | TBR2 h | TBR4 h | |
| 1 | 61 | Right primary | +++ | +++ | 10 | 5 | 7.33 | 0.89 | 0.81 | 5 | 0 | 2.00 | 0.82 | 0.77 | Stable disease |
| | | M | | | | | 4.30 | 0.73 | 0.63 | | | 0.90 | 0.27 | 0.43 | PR |
| 2 | 55 | Left M | ++ | − | 24 | | 8.02 | 1.13 | 1.20 | | | 7.10 | 1.58 | 1.83 | PD |
| | | M | ++ | − | 10 | | 9.65 | 0.92 | 1.09 | | | 4.10 | 1.18 | 1.12 | Stable disease |
| 3 | 74 | Left primary | ++ | ++ | 10 | 5 | 2.74 | 1.27 | 1.31 | 15 | 5 | 2.84 | 1.34 | 1.41 | PD |
| 4 | 65 | Right primary | +++ | ++ | 20 | | 8.26 | 1.03 | 1.05 | 5 | 1 | 8.26 | 0.98 | 0.84 | PR |
| 5 | 56 | Left M | ++ | + | 30 | 4 | 6.10 | 1.62 | 1.31 | | | 6.70 | 0.88 | 1.11 | PD |
| 6 | 56 | Left primary | +++ | +++ | 40 | 4 | 7.61 | 1.25 | 1.50 | 5 | 4 | 4.60 | 0.80 | 0.91 | Stable disease |
| | | M | | | | | 6.70 | 0.62 | 0.66 | | | 3.30 | 0.29 | 0.21 | PR |
| 7 | 74 | Left primary | ++ | ++ | 20 | 5 | 3.20 | 0.81 | 0.89 | 1 | 5 | 3.20 | 0.73 | 0.88 | PR |
| 8 | 58 | M | +++ | +++ | 15 | | 7.10 | 1.66 | 2.29 | | | 13.04 | 1.83 | 2.15 | PD |
| 9 | 74 | Right primary | +++ | +++ | 75 | | 1.40 | 0.80 | 1.10 | 5 | | 3.40 | 0.50 | 0.90 | Stable disease |
| 10 | 70 | Right primary | +++ | +++ | 50 | | 2.90 | 1.18 | 1.18 | 5 | | 1.60 | 0.90 | 1.15 | PR |
| | | M1 | | | | | 4.50 | 1.03 | 1.06 | | | 12.80 | 1.14 | 1.14 | PR |
| | | M2 | | | | | 3.83 | 0.90 | 0.94 | | | 1.58 | 0.88 | 1.01 | PR |
| 11 | 64 | M1 | ++ | ++ | 50 | | 8.00 | 1.38 | 1.87 | | | 11.50 | 1.77 | 2.05 | PD |
| | | M2 | | | | | 12.20 | 1.18 | 1.27 | | | 11.10 | 1.97 | 2.28 | PD |
| | | M3 | | | | | 10.90 | 1.14 | 1.27 | | | 6.50 | 1.63 | 1.55 | PD |
| | | M4 | | | | | 13.49 | 1.02 | 1.34 | | | 10.10 | 1.17 | 1.03 | PD |
| | | M5 | | | | | 8.74 | 1.19 | 1.14 | | | 7.90 | 1.31 | 1.16 | PD |
| 12 | 55 | Right primary | +++ | +++ | 30 | | 5.45 | 1.23 | 1.30 | | | | | | PD |
| | | M1 | | | | | 4.50 | 1.98 | 1.65 | | | | | | PD |
| | | M2 | | | | | 4.00 | 1.39 | 0.93 | | | | | | PD |
| | | M3 | | | | | 5.80 | 1.55 | 2.26 | | | | | | PD |
| | | M4 | | | | | 6.67 | 3.07 | 1.89 | | | | | | PD |
| | | M5 | | | | | 6.18 | 1.29 | 1.79 | | | | | | PD |
| | | M6 | | | | | 5.17 | 1.60 | 1.63 | | | | | | PD |
| | | M7 | | | | | 5.81 | 1.93 | 1.57 | | | | | | PD |
| 13 | 58 | Left primary | +++ | +++ | 20 | | 4.50 | 0.76 | 0.80 | | | | | | PR |
| | | M | | | | | 4.40 | 0.72 | 0.67 | | | | | | PR |
| 14 | 82 | Left primary | +++ | +++ | | | 3.93 | 1.06 | 1.02 | | | | | | PR |
| 15 | 67 | Left primary | +++ | +++ | 5 | 4 | 6.60 | 0.83 | 0.88 | | | | | | PR |
| 16 | 59 | Left primary | +++ | +++ | | 4 | 2.46 | 0.72 | 0.95 | | | | | | Stable disease |
| 17 | 78 | Left primary | +++ | +++ | | | | | | 15 | 5 | 4.50 | 0.86 | 0.76 | PR |
| 18 | 60 | M1 | +++ | +++ | | | | | | | | 5.60 | 0.99 | 0.91 | Stable disease |
| | | M2 | | | | | | | | | | 4.30 | 0.88 | 0.80 | Stable disease |
| | | M3 | | | | | | | | | | 6.80 | 1.01 | 0.93 | Stable disease |
| | | M4 | | | | | | | | | | 8.20 | 1.12 | 1.28 | Stable disease |
| | | M5 | | | | | | | | | | 7.62 | 1.10 | 1.06 | Stable disease |

**TABLE 1 (Continued)**

| Patient no | Age (y) | Diagnoses | Baseline | | | | | | | Follow-up | | | | Outcome |
|---|---|---|---|---|---|---|---|---|---|---|---|---|---|---|
| | | | EP | PR | Ki67 (%) | HIF-1α score | SUVFDGpeak | TBR2 h | TBR4 h | Ki67 (%) | HIF-1α score | SUVFDG peak | TBR2 h | TBR4 h | |
| 19 | 77 | M1 | +++ | ++ | | | | | | 85 | | 9.58 | 1.04 | 1.98 | PD |
| | | M2 | | | | | | | | | | 6.74 | 0.94 | 0.98 | PD |
| | | M3 | | | | | | | | | 5 | 8.20 | 1.14 | 1.40 | PD |
| 20 | 59 | M1 | | | | | | | | | | 12.90 | 1.08 | 1.11 | PD |
| | | M2 | +++ | ++ | | | | | | | | 13.35 | 1.03 | 1.31 | PD |
| | | M3 | | | | | | | | | | 8.40 | 1.86 | 1.61 | PD |

+++ = strong positive; ++ = intermediate positive; − = negative; + = weak positive; M = metastasis.

ymy and in the opposite side. The mean value of 6 background VOI peaks was noted as SUV2 $h_B$, TBR2 h = SUV2 $h_T$/SUV2 $h_B$, and TBR4 h = SUV4 $h_T$/SUV4 $h_B$ (TBR is the tumor-to-background ratio).

### Tissue Specimens and Immunohistochemistry

Each patient underwent diagnostic core-needle biopsy on the primary site at baseline. A therapeutic surgery (quadrantectomy or mastectomy in association with sentinel node biopsy or axillary node dissection) or a second core-needle biopsy on the primary site was planned in a subset of patients after at least 3 mo of primary letrozole therapy. Both biopsy and surgical samples of primary tumors were routinely embedded in paraffin wax and cut to 3- to 5-μm thickness and dried overnight at 37°C for immunohistochemistry testing. Immunohistochemistry staining for HIF-1α (Novus Biologicals) was performed on 3- to 5-μm serial sections on coated slides. After the slides were dried at 80°C overnight, they were dewaxed in xylene (10 min, 3 times) and rehydrated using graded alcohol. Antigens were retrieved by cooking in Tris (pH 6.0). The mouse monoclonal antibody H1α67 (at a dilution of 1:100 in tris-buffered saline with 10% normal bovine serum) was used to assess the expression of HIF-1α and incubated overnight at 4°C. Next, an hour-long incubation with a Supervision Universal (antimouse–antirabbit) Detection Reagent (Dako) (horseradish peroxidase) was performed. Slides were then stained with 3,3′-diaminobenzidine chromogen solution for 10 min and then counterstained with hematoxylin and mounted with Aquamount. Immunohistochemistry staining for Ki67 was performed on an automated immunohistochemistry stainer at room temperature. Known positive and negative controls (obtained by omission of primary antibodies) were used to ensure quality control of staining.

All immunohistochemistry slides were examined by light microscopy by 2 observers masked to patient outcome. The HIF-1α level was assessed within the entire tumor section with a semiquantitative scale that combined proportional expression (scored as 0, no expression; 1, <10%; 2, 10%–50%; 3, 50%–80%; and 4, >80% of cells showing nuclear staining) and staining intensity(scored as 0, none; 1, weak; 2, intermediate; and 3, strong) to obtain an a total immunohistochemistry score from 0 to 7 (*22*). Ki-67 was scored as the percentage of positively stained cells among 1,000 malignant cells.

### Statistical Analysis

Data were analyzed using SPSS software (version 17.0; SPSS–IBM). We tested the hypothesis that $^{18}$F-FDG and $^{18}$F-FMISO uptake in breast tumors was correlated with response to primary endocrine therapy. The Pearson correlation coefficient was computed to determine the correlation among the hottest spot in the tumor foci ($SUV_{FDGpeak}$), SUV2 $h_T$, SUV4 $h_T$, TBR2 h, and TBR4 h. Spearman rank correlation was used to determine the correlation among 3 groups (complete and partial responders [PRs], stable disease, and progressive disease [PD]) and $^{18}$F-FDG/$^{18}$F-FMISO uptake with a 0.01 threshold for statistical significance. The optimal cutoff value was selected according to PD and PR. Other tests were performed to answer the question of whether $^{18}$F-FDG or $^{18}$F-FMISO uptake correlates with expression of either HIF-1α or Ki67.

## RESULTS

Forty-five lesions (13 primary, 32 metastasis) from 20 patients met the inclusion criteria of the study, including 13 primary sites of breast cancer, 20 regional lymph node

metastases, 8 local recurrences, and 4 lung and pleura metastases.

### $^{18}$F-FDG/$^{18}$F-FMISO Uptake in Primary and Metastatic Lesions

Twenty lesions from 11 patients (patients 1–11) underwent both baseline and follow-up $^{18}$F-FDG/$^{18}$F-FMISO PET/CT scans. Thirteen lesions from 5 patients (patients 12–16) underwent baseline scans only, and the remaining 12 lesions from 4 patients (patients 17–20) underwent follow-up scans only. Therefore, 65 PET/CT scans for 45 lesions were eligible for analysis (Table 1). The $SUV_{FDGpeak}$ of these sixty-five $^{18}$F-FDG PET/CT scans ranged from 0.90 to 13.49 (mean, 6.40 ± 3.44). For $^{18}$F-FMISO PET/CT scans, SUV2 $h_T$ ranged from 0.48 to 4.76 (mean, 1.85 ± 0.69); SUV4 $h_T$ ranged from 0.48 to 3.52 (mean, 1.80 ± 0.67), TBR2 h ranged from 0.27 to 3.07 (mean, 1.15 ± 0.45), and TBR4 h ranged from 0.21 to 2.29 (mean, 1.22 ± 0.45). There were weaker correlations for $SUV_{FDGpeak}$ versus SUV4 $h_T$ ($r = 0.46$) and $SUV_{FDGpeak}$ versus TBR4 h ($r = 0.44$). However, strong correlations were found for SUV2 $h_T$ versus SUV4 $h_T$, TBR2 h versus TBR4 h, SUV2 $h_T$ versus TBR4 h, and SUV4 $h_T$ versus TBR4 h ($r = 0.77$, 0.79, 0.79, and 0.94, respectively; $P < 0.0001$ for all). $SUV_{FDGpeak}$, TBR2 h, and TBR4 h were all greater for metastatic lesions than for primary lesions, and the differences were significant ($t = 4.51$, 3.49, and 3.23, respectively, $P < 0.01$ for all).

### Predictive Value of $^{18}$F-FDG/$^{18}$F-FMISO

In the current study, baseline $^{18}$F-FMISO PET/CT scans were performed on 33 lesions from 16 patients (Table 1, patients 1–16). After more than 3 mo of treatment with letrozole, 0 lesions were considered complete responders, 11 were PRs, 5 were stable disease, and 17 were PD (Figs. 1 and 2).The correlation between $SUV_{FDGpeak}$ and clinical outcome was weak and did not reach statistical significance ($r = 0.37$, $P = 0.031$). However, there was a significantly positive correlation between baseline $^{18}$F-FMISO uptake (SUV2 $h_T$, TBR2 h, SUV4 $h_T$, and TBR4 h) and clinical outcome ($r = 0.77$, 0.76, 0.71, and 0.78, respectively; $P < 0.0001$). Application of a cutoff of TBR4 h ≥ 1.2 allowed prediction of 88% of PDs (15/17), whereas cutoffs of TBR2 h ≥ 1.2, SUV2 $h_T$ ≥ 2.1, and SUV4 $h_T$ ≥ 2.1 identified 70% (12/17), 64% (11/17), and 64% (11/17) of PDs, respectively. However, $SUV_{FDGpeak}$ could not predict PD or PRs because a clear cutoff could not be defined (Figs. 3A–3C). After at least 3 mo of follow-up, 20 of 33 lesions underwent an additional $^{18}$F-FMISO PET/CT scan. Comparing TBR4 h at baseline and at follow-up indicated that TBR4 h in PRs and stable disease shows a decreasing trend; in contrast, TBR4 h in PD did not follow this same trend (Fig. 3D).

### Relationship Between $^{18}$F-FDG/$^{18}$F-FMISO Uptake and HIF-1α and Ki67

As shown in Table 1, HIF-1α and Ki67 expression were detected by immunohistochemistry in 14 and 22 samples, respectively. No correlation was found between $^{18}$F-FDG/$^{18}$F-FMISO uptake and HIF-1α expression ($r = 0.01$ and 0.34, respectively; $P = 0.81$ and 0.62, respectively). Ki67 did not correlate with $SUV_{FDGpeak}$, SUV2 $h_T$, or TBR2 h ($r = 0.23$, 0.28, and 0.25, respectively; and $P = 0.27$, 0.19, and 0.23, respectively). There was a marginal correlation between Ki67 expression and TBR4 h ($r = 0.51$, $P = 0.011$).

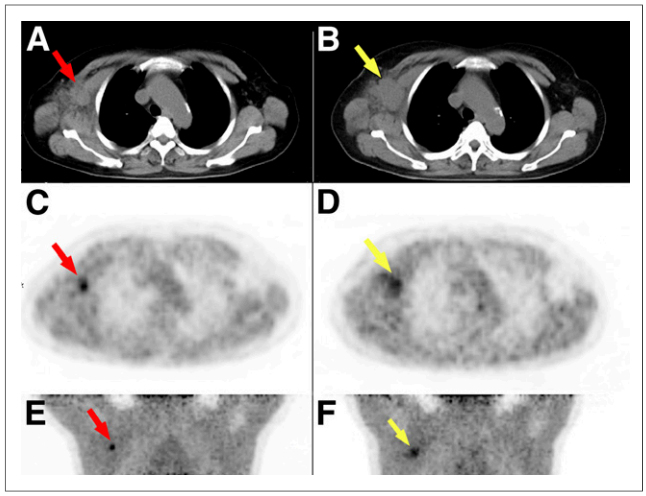


**FIGURE 1.** Metastatic right axillary node in patient 8. Metastatic lesion (23 × 17 mm) showed high $^{18}$F-FMISO uptake at baseline (red arrow) (TBR4 h = 2.29). After more than 3 mo of treatment with letrozol, metastatic lesion progressed (30 × 20 mm) and still revealed high $^{18}$F-FMISO uptake (yellow arrow) (TBR4 h = 2.15). (A) CT image in baseline. (B) CT image in follow-up. (C) PET image in baseline. (D) PET image in follow-up. (E) Maximum-intensity-projection image in baseline. (F) Maximum-intensity-projection image in follow-up.

## DISCUSSION

Endocrine therapy is suitable for both primary and recurrent/metastatic hormone receptor (ER)–positive breast

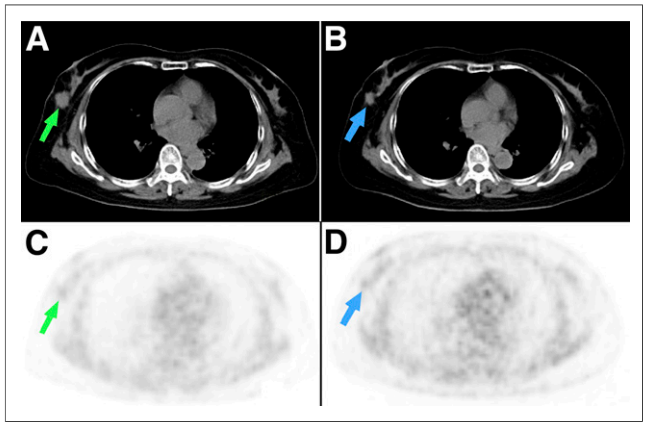


**FIGURE 2.** Right breast tumor in patient 4. Primary lesion (19 × 18 mm) did not show decreased $^{18}$F-FMISO uptake at baseline (green arrow) (TBR4 h = 1.05). After more than 3 mo of treatment with letrozole, primary lesion lessened (11 × 10 mm) and still had no decreased $^{18}$F-FMISO uptake (blue arrow) (TBR4 h = 0.84). (A) CT image in baseline. (B) CT image in follow-up. (C) PET image in baseline. (D) PET image in follow-up.

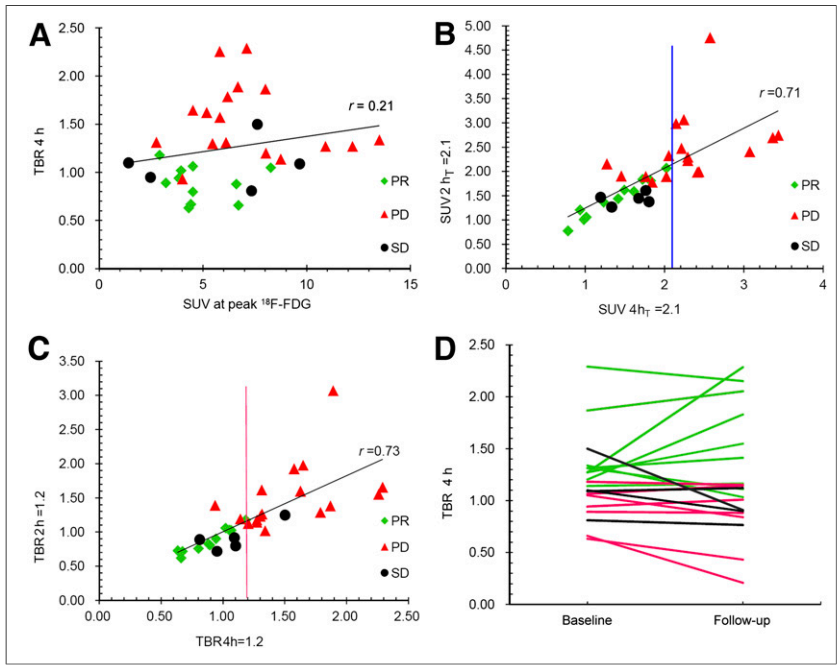


**FIGURE 3.** Application of cutoff TBR4 h of ≥ 1.2 allowed prediction of 88% (15/17) PDs and all PRs (C) Although using SUV4hT ≥ 2.1 could identify 64% (11/17) of PDs and all PRs (B), SUVFDGpeak could not predict PDs and PRs because clear cutoff could not be defined (A). When TBR4 h in baseline and follow-up were compared, TBR4 h in stable disease and PRs showed downtrend, whereas TBR4 h in PDs did not (D). SD = stable disease.

cancer. Unfortunately, however, not all women respond to treatment. The preoperative endocrine prognostic index is a comprehensive evaluation score based on multiple parameters, including histopathologic tumor size after 3–4 mo of primary endocrine therapy, nodal status, ER levels, and Ki67 levels. The index can be used as a tool for individualization of primary endocrine therapy (*23*). Unfortunately, according to the preoperative endocrine prognostic index, approximately 30%–40% of patients with primary resistance to hormonal therapy receive unnecessary treatment. As a result, their conditions may even worsen. It has been reported that Ki67 levels measured after a short term (2 wk) of neoadjuvant endocrine therapy can predict long-term outcome for individual patients (*24*), and the same may be true for pretreatment HIF-1α levels (*9,10*). However, it is difficult to obtain biopsies of metastatic lesions in patients with advanced breast cancer. Thus, it is urgent and valuable to find a noninvasive means with the same efficacy as histopathologic marker analysis to predict primary hormonal therapy resistance. Our study revealed that $^{18}$F-FMISO PET/CT is a highly effective method that can accurately predict the clinical efficacy of primary endocrine therapy and has a marginal positive correlation with Ki67 levels.

For over a decade, $^{18}$F-FMISO has been used as a PET tracer for hypoxia imaging of several solid tumors, including non–small cell lung cancer (NSCLC), head and neck cancer, soft-tissue sarcomas, and renal cell carcinoma. To our knowledge, no study has examined the role of $^{18}$F-FMISO PET/CT in predicting endocrine resistance in breast cancer. Therefore, no previous studies could provide optimal parameters and cutoffs. Here, we found that TBR4 h is an optimal parameter to assess the degree of hypoxia; importantly, this finding agrees with earlier reports (*25,26*). The tumor VOI was delineated using $^{18}$F-FDG image data in 3-dimensional mode with TrueD software to obtain the $SUV_{FDGpeak}$—the hottest spot in the tumor. The back muscle was chosen as reference in both homonymy and opposite side because the distribution and drainage of tracer in homonymy muscles may be affected after surgery and radiotherapy. As a result, we drew 6 background VOIs to obtain the average background VOI, which was more representative and close to real for analysis. Each tumor may have its own cutoff threshold because blood supply, location, and extent of necrosis vary from tumor to tumor. For example, 1.2 is a cutoff value for head and neck cancer and soft-tissue sarcomas (*18,27,28*), 1.24 is a cutoff value for nasopharyngeal carcinoma (*29*), and 1.4 is the cutoff for NSCLC because the unique structure of the lung parenchyma, including its dual blood supply and abundant oxygen-containing air space, may play a role in NSCLC's being less hypoxic than other tumor types (*30,31*). In our study, 16 patients with 33 lesions underwent hypoxia detection at baseline, which was then used to predict endocrine therapy outcome. We determined cutoff values according to clinical responses previously reported in the literature (*15*) to ensure no false-positives were included. In our patients, a TBR4 h ≥ 1.2 can predict 88% of PDs and 100% of PRs. It is better than other parameters (TBR2 h, SUV2 $h_T$, and SUV4 $h_T$) and still correlates well with them.

Under normal conditions, hypoxia can greatly enhance glucose uptake through upregulation of glycolytic enzymes. The results of our study show that $SUV_{FDGpeak}$ does not correlate with either $^{18}$F-FMISO uptake or with the efficacy of endocrine therapy, suggesting that the alteration of glucose metabolism in breast cancer cells characterized by

a preference of aerobic glycolysis, known as the Warburg effect, appears to be caused by more than hypoxia and has no relationship with endocrine therapy resistance. Thus, the relationship between hypoxia and endocrine therapy resistance needs further examination.

Like $SUV_{FDGpeak}$, HIF-1α did not correlate with $^{18}$F-FMISO uptake in our study. This finding is in line with earlier studies (*32–35*). HIF-1α was mainly expressed in the cytoplasm (90%–100%) and was highly sensitive to oxygen partial pressure. Many procedures such as surgery and sample collection could cause artificial hypoxia, leading to increased HIF-1α expression and a high false-positive rate. It was noted that not only in hypoxia but also under normal oxygen concentrations, HIF-1α can be induced by a variety of stimuli, such as growth factors, cytokines, hormones, and viral proteins. These pathways are often upregulated in tumor cells because of the activation of oncogenes and loss of tumor suppressors, notably phosphatase and tensin homolog deleted on chromosome 10, von Hippel-Lindau protein, and p53 (*36*,*37*). Another reason for the discrepancy between HIF-1α expression and $^{18}$F-FMISO uptake may be that the fluctuation of tumor oxygenation at pO2 levels of 10 mm Hg or more would not be detected by $^{18}$F-FMISO PET/CT scans but could nevertheless lead to the activation of the HIF system (*34*). Ki67 has been used as a tumor marker to predict response to endocrine therapy. The expression level of Ki67 had been reported to be negatively correlated with clinical outcome (*24*). In theory, an increase in cellular proliferation should be accompanied by an increase in oxygen supply. When the oxygen supply cannot adequately meet the needs of locally advanced tumors, hypoxia will likely develop. Our study reveals a marginal correlation between Ki67 expression and $^{18}$F-FMISO uptake and retention ($r = 0.51$, $P = 0.012$, and $r = 0.51$, $P = 0.011$, respectively). However, there was no correlation between Ki67 expression and $^{18}$F-FDG uptake ($r = 0.23$, $P = 0.27$). Similar results were reported for NSCLC, in which only a weak positive correlation between $^{18}$F-FMISO uptake and Ki67 was found (*30*). It is possible that hypoxia in breast tumors does not depend on cellular proliferation and could be an independent predictive factor of clinical outcome.

We find that the state of hypoxia in ER-positive breast tumors at baseline could predict resistance to endocrine therapy. The prognostic value of $^{18}$F-FMISO PET/CT performed at baseline will be assessed in future studies with more patients.

## CONCLUSION

Monitoring the effects of endocrine therapy is critical to determine whether the current treatment should be continued, stopped, or changed to a more aggressive regimen. An effective method for monitoring the response to endocrine therapy is needed to ensure early identification of nonresponders. Our study used a noninvasive and repeatable method, $^{18}$F-FMISO PET/CT, to predict the outcome after endocrine therapy and confirm that TBR4 h $\geq$ 1.2 is an optimal cutoff that highly suggests resistance to hormonal therapy.

## DISCLOSURE

The costs of publication of this article were defrayed in part by the payment of page charges. Therefore, and solely to indicate this fact, this article is hereby marked "advertisement" in accordance with 18 USC section 1734. This research is supported by the Shanghai Committee of Science and Technology, China (grant 12DZ2260100), and by grants from the National Natural Science Foundation of China (30600725), the Shanghai United Developing Technology Project of Municipal Hospitals (SHDC12010116), the Key Clinical Program of the Ministry of Health (2010-2012), and Novartis. The research funders had no role in study design, data collection and analysis, decision to publish, or preparation of the manuscript. No other potential conflict of interest relevant to this article was reported.

## ACKNOWLEDGMENTS

We thank all the subjects of this study for their participation. We greatly appreciate Hong-Fen Lu, Xue-Ke Zhou and Xu Cai at Department of Pathology of Shanghai Cancer Center for their excellent work in Immunohisto-chemistry testing.

## REFERENCES

1. Mouridsen H, Gershanovich M, Sun Y, et al. Superior efficacy of letrozole versus tamoxifen as first-line therapy for postmenopausal women with advanced breast cancer: results of a phase III study of the International Letrozole Breast Cancer Group. *J Clin Oncol.* 2001;19:2596–2606.
2. Ellis MJ, Coop A, Singh B, et al. Letrozole inhibits tumor proliferation more effectively than tamoxifen independent of HER1/2 expression status. *Cancer Res.* 2003;63:6523–6531.
3. Bunn HF, Poyton RO. Oxygen sensing and molecular adaptation to hypoxia. *Physiol Rev.* 1996;76:839–885.
4. Vaupel P, Hoeckel M. Predictive power of the tumor oxygenation status. *Adv Exp Med Biol.* 1999;471:533–539.
5. Bos R, Groep P, Greijer AE, et al. Levels of hypoxia-inducible factor-1α independently predict prognosis in patients with lymph node negative breast carcinoma. *Cancer.* 2003;97:1573–1581.
6. Aebersold DM, Burri P, Beer KT, et al. Expression of hypoxia-inducible factor-1alpha: a novel predictive and prognostic parameter in the radiotherpy of oropharyngeal cancer. *Cancer Res.* 2001;61:2911–2916.
7. Kurebayashi J, Otsuki T, Moriya T, et al. Hypoxia reduces hormone responsiveness of human breast cancer cells. *Jpn J Cancer Res.* 2001;92:1093–1101.
8. Cooper C, Liu GY, Niu YL, et al. Intermittent hypoxia induces proteasome-dependent down-regulation of estrogen receptor alpha in human breast carcinoma. *Clin Cancer Res.* 2004;10:8720–8727.
9. Generali D, Berruti A, Brizzi MP, et al. Hypoxia-inducible factor-1alpha expression predicts a poor response to primary chemoendocrine therapy and disease-free survival in primary human breast cancer. *Clin Cancer Res.* 2006;12:4562–4568.
10. Generali D, Buffa FM, Berruti A, et al. Phosphorylated ER-alpha, HIF-1α, and MAPK signaling as predictors of primary endocrine treatment response and resistance in patients with breast cancer. *J Clin Oncol.* 2009;27:227–234.
11. Vaupel P, Schlenger K, Knoop C, et al. Oxygenation of human tumors: evaluation of tissue oxygen distribution in breast cancer by computerized O2 tension measurements. *Cancer Res.* 1991;51:3316–3322.
12. Lee ST, Scott AM. Hypoxia positron emission tomography imaging with 18f-fluoromisonidazole. *Semin Nucl Med.* 2007;37:451–461.

13. Rasey JS, Nelson NJ, Chin L, et al. Characteristics of the binding of labeled fluoromisonidazole in cells in vitro. *Radiat Res.* 1990;122:301–308.
14. Valk PE, Mathis CA, Prados MD, et al. Hypoxia in human gliomas: demonstration by PET with fluorine-18-fluoromisonidazole. *J Nucl Med.* 1992;33:2133–2137.
15. Eschmann SM, Paulsen F, Reimold M, et al. Prognostic impact of hypoxia imaging with $^{18}$F-misonidazole PET in non-small cell lung cancer and head and neck cancer before radiotherapy. *J Nucl Med.* 2005;46:253–260.
16. Gagel B, Reinartz P, Demirel C, et al. [$^{18}$F]fluoromisonidazole and [$^{18}$F]fluorodeoxyglucose positron emission tomography in response evaluation after chemo-/radiotherapy of non-small-cell lung cancer: a feasibility study. *BMC Cancer.* 2006;6:51.
17. Vaupel P, Thews O, Hoeckel M. Treatment resistance of solid tumors: role of hypoxia and anemia. *Med Oncol.* 2001;18:243–259.
18. Lawrentschuk N, Poon AM, Foo SS, et al. Assessing regional hypoxia in human renal tumours using $^{18}$F-fluoromisonidazole positron emission tomography. *BJU Int.* 2005;96:540–546.
19. Gagel B, Reinartz P, Dimartino E, et al. pO(2) Polarography versus positron emission tomography ([$^{18}$F] fluoromisonidazole, [$^{18}$F]-2-fluoro-2=-deoxyglucose): an appraisal of radiotherapeutically relevant hypoxia. *Strahlenther Onkol.* 2004;180:616–622.
20. Zimny M, Gagel B, Dimartino E, et al. FDG: a marker of tumour hypoxia? A comparison with [$^{18}$F]fluoromisonidazole and pO (2)-polarography in metastatic head and neck cancer. *Eur J Nucl Med Mol Imaging.* 2006;33:1426–1431.
21. World Health Organization. *World Health Organization, WHO Handbook for Reporting Results of Cancer Treatment*. Geneva, Switzerland: World Health Organization; 1978.
22. Birner P, Schindl M, Obermair A, Breitenecker G, Oberhuber G. Expression of hypoxia-inducible factor 1alpha in epithelial ovarian tumors: its impact on prognosis and on response to chemotherapy. *Clin Cancer Res.* 2001;7:1661–1668.
23. Ellis MJ, Tao Y, Luo J, et al. Outcome prediction for estrogen receptor-positive breast cancer based on postneoadjuvant endocrine therapy tumor characteristics. *J Natl Cancer Inst.* 2008;100:1380–1388.
24. Dowsett M, Smith IE, Ebbs SR, et al. Prognostic value of Ki67 expression after short-term presurgical endocrine therapy for primary breast cancer. *J Natl Cancer Inst.* 2007;99:167–170.
25. Nunn A, Linder K, Strauss HW, et al. Nitroimidazoles and imaging hypoxia. *Eur J Nucl Med.* 1995;22:265–280.
26. Padhani AR, Krohn KA, Lewis JS, et al. Imaging oxygenation of human tumours. *Eur Radiol.* 2007;17:861–872.
27. Rasey JS, Koh WJ, Evans ML, et al. Quantifying regional hypoxia in human tumors with positron emission tomography of [$^{18}$F]fluoromisonidazole: a pretherapy study of 37 patients. *Int J Radiat Oncol Biol Phys.* 1996; 36:417–428.
28. Rajendran JG, Wilson DC, Conrad EU, et al. [$^{18}$F]FMISO and [$^{18}$F]FDG PET imaging in soft tissue sarcomas: Correlation of hypoxia,metabolism and VEGF expression. *Eur J Nucl Med Mol Imaging.* 2003;30:695–704.
29. Yeh SH, Liu RS, Wu LC, et al. Fluorine-18 fluoromisonidazole tumour to muscle retention ratio for the detection of hypoxia in nasopharyngeal carcinoma. *Eur J Nucl Med.* 1996;23:1378–1383.
30. Cherk MH HC, Serene SF, Aurora MTP, et al. Lack of correlation of hypoxic cell fraction and angiogenesis with glucose metabolic rate in non–small cell lung cancer assessed by $^{18}$F-fluoromisonidazole and $^{18}$F-FDG PET. *J Nucl Med.* 2006;47:1921–1926.
31. Le QT, Chen E, Salim A, et al. An evaluation of tumor oxygenation and gene expression in patients with early stage non-small cell lung cancers. *Clin Cancer Res.* 2006;12:1507–1514.
32. Mayer A, Hockel M, Wree A, et al. Microregional expression of glucose transporter-1 and oxygenation status: lack of correlation in locally advanced cervical cancers. *Clin Cancer Res.* 2005;11:2768–2773.
33. Vordermark D, Brown JM. Evaluation of hypoxia-inducible factor-1_(HIF-1_) as an intrinsic marker of tumor hypoxia in U87 MG human glioblastoma: in vitro and xenograft studies. *Int J Radiat Oncol Biol Phys.* 2003;56:1184–1193.
34. Cárdenas-Navia LI. The pervasive presence of fluctuating oxygenation in tumors. *Cancer Res.* 2008;68:5812–5819.
35. Lehmann S, Stiehl DP, Honer M, et al. Longitudinal and multimodal in vivo imaging of tumor hypoxia and its downstream molecular events. *Proc Natl Acad Sci USA.* 2009;106:14004–14009.
36. Zundel W, Schindler C, Haas-Kogan D, et al. Loss of PTEN facilitates HIF-1-mediated gene expression. *Genes Dev.* 2000;14:391–396.
37. Pouyssegur J, Dayan F, Mazure NM. Hypoxia signalling in cancer and approaches to enforce tumor regression. *Nature*. 2006;441:437–443.

The Journal of NUCLEAR MEDICINE

# $^{18}$F-Fluoromisonidazole PET/CT: A Potential Tool for Predicting Primary Endocrine Therapy Resistance in Breast Cancer

Jingyi Cheng, Li Lei, Junyan Xu, Yifei Sun, Yongping Zhang, Xincun Wang, Lingling Pan, Zhimin Shao, Yingjian Zhang and Guangyu Liu

*J Nucl Med.* 2013;54:333-340.
Published online: February 11, 2013.
Doi: 10.2967/jnumed.112.111963



*The Journal of Nuclear Medicine* is published monthly.
SNMMI | Society of Nuclear Medicine and Molecular Imaging
1850 Samuel Morse Drive, Reston, VA 20190.
(Print ISSN: 0161-5505, Online ISSN: 2159-662X)



SNMMI SOCIETY OF NUCLEAR MEDICINE AND MOLECULAR IMAGING